

# EVALUATION OF THE MATERIAL RELEASE FROM A CYLINDRICAL WASTE FORM VIA LAPLACE TRANSFORMS

B. D. Ganapol  
 Department of Nuclear and Energy Engineering  
 University of Arizona  
 Tucson, Arizona 85721

## ABSTRACT

A new method for determining the material release fraction and release rate from a cylindrical waste form is presented. The method employs a numerical Laplace transform inversion and generates accurate results for intermediate and small times after the initiation of the release. Asymptotic expressions valid at short times are also obtained and used in a comparison of model and test data.

## INTRODUCTION

The initial phase of either long-term interim storage or final disposal of high level nuclear waste is the encapsulation of the waste in a solid matrix. In most instances, a cylindrical container seems to be the most convenient form of the matrix for storage purposes. Thus at the heart of an analysis to determine the potential for radioactive release from a repository lies the evaluation of the diffusional release characteristics of a cylindrical waste container. Previous attempts to investigate leaching from waste forms have considered these forms to be either semi-infinite media or one-dimensional. Recently, Nestor (1) and later Thomas (2) have presented analytical methods for determining the leached fractional inventory (f) and leaching rate (g) as functions of time (t) from a finite cylindrical waste form. The resulting expressions obtained by Thomas involve double infinite series which seem to be rather difficult to evaluate to a high degree of accuracy at small times. Thomas therefore proposes a rather ad-hoc numerical procedure involving an additional integration and expansion in Bernoulli numbers which apparently allows one to evaluate the resulting double sum, although, no evidence is presented to substantiate this claim. An alternative and more straightforward method of evaluation will be investigated here.

In the presentation to follow, both f and g will be evaluated using either a numerical Laplace transform inversion that avoids the double summation entirely or an asymptotic expression. In effect, the Laplace transformed diffusion equation is solved analytically in two-dimensional cylindrical geometry and the result is numerically inverted on the Bromwich contour thus avoiding analytically continuing the transform into the complex plane. It must be emphasized that the main focus of this work at this stage of development is the presentation of the method of numerical inversion and is not its application to realistic waste storage scenarios. As demonstrated, the main use of the method is to provide accurate comparative results for waste forms of different diffusional and absorptive characteristics to be used in design and assessment.

## THEORY

The appropriate diffusion equation for a single component diffusing from a cylindrical waste form with azimuthal symmetry shown in Fig. 1 is

$$\left[ D \left( \frac{\partial^2}{\partial \rho^2} + \frac{1}{\rho} \frac{\partial}{\partial \rho} + \frac{\partial^2}{\partial z^2} \right) - k \right] c(\rho, z, t) = \frac{\partial}{\partial t} c(\rho, z, t) \quad (1)$$

where D is the material diffusivity, k is a loss rate coefficient modelling decay and retention in the waste form and c is the diffusant concentration. After a Laplace transformation and solution of the resulting equation, we find (2) assuming D and k are constants

$$\bar{c}(\rho, z, s) = \frac{2c_0}{D} \sum_{m=1}^{\infty} \frac{(-1)^{m-1}}{\mu_m^2 \beta_m} \left[ 1 - \frac{I_0(\mu_m \rho)}{I_0(\mu_m a)} \right] \cos(\beta_m z) \quad (2)$$

where  $c_0$  is the initial uniform concentration and

$$\beta_m = \pi(2m-1)/2\ell$$

$$\mu_m^2 = (s+k+\beta_m^2 D)/D$$

$I_n$  = modified Bessel function of order n

The transform of the fractional inventory of continuously leached material from the waste form is therefore given by the transform of the flux at the cylinder boundaries

$$\bar{f}(s, k) = \frac{2}{s} (a^2 \ell c_0)^{-1} \left[ \int_0^a d\rho \rho \left( -D \frac{d\bar{c}}{dz} \right)_{z=\ell} + \int_0^{\ell} dz \left( -D \frac{\partial \bar{c}}{\partial \rho} \right)_{\rho=a} \right] \quad (3a)$$

with the corresponding transform of the leaching rate

$$\bar{g}(s, k) = s \bar{f}(s, k) \quad (3b)$$

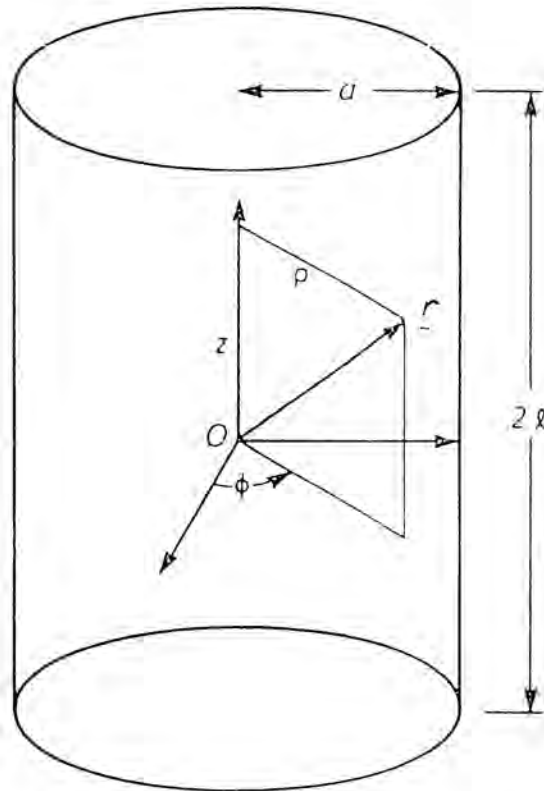


Fig. 1. Cylindrical Waste Form.

From the application of the Laplace transform inversion to Eqs. (2) and (3), the following expressions for f and g result:

$$f(t,0) = 1 - \frac{2}{\ell^2} \sum_{m=1}^{\infty} \frac{e^{-D\beta_m^2 t}}{\beta_m^2} + \frac{4}{\ell^2} \int_0^{\tau} \left\{ \frac{1}{s^{3/2}} \frac{I_1(s^{1/2})}{I_0(s^{1/2})} \right\} \sum_{m=1}^{\infty} \frac{e^{-D\beta_m^2 t}}{\beta_m^2} \quad (5)$$

$$f(t,k) = 1 - \frac{2}{\ell^2} \sum_{m=1}^{\infty} \frac{1}{(B_m^2 + k/D)} \left[ \frac{k/D}{\beta_m^2} + e^{-(D\beta_m^2 + k)t} \right] + \frac{4}{\ell^2} \sum_{m=1}^{\infty} \frac{1}{\beta_m^2} \int_0^{\tau} \left\{ \frac{1}{\mu_m a} (s + D\beta_m^2 + k)^{-1} (1+k/s) \frac{I_1(\mu_m a)}{I_0(\mu_m a)} \right\} \quad (4a)$$

where

$$\tau = Dt/a^2$$

and

$$g(t,k) = e^{-kt} \left[ \frac{2D}{\ell^2} \sum_{m=1}^{\infty} e^{-\beta_m^2 Dt} + \frac{4}{\ell^2 a} \sum_{m=1}^{\infty} \frac{1}{B_m^2} \int_0^{\tau} \left\{ \frac{s}{\mu'_m (s + D\beta_m^2)} \frac{I_1(\mu'_m a)}{I_0(\mu'_m a)} \right\} \right] \quad (4b)$$

where

$$\mu'_m{}^2 \equiv (s + D\beta_m^2)/D$$

Similarly, for any k, the expression for g can be reduced to

$$g(t,k) = e^{-kt} \frac{2D}{\ell^2} \left\{ \left[ 1 - 2 \int_0^{\tau} \left\{ \frac{1}{s^{3/2}} \frac{I_1(s^{1/2})}{I_0(s^{1/2})} \right\} \sum_{m=1}^{\infty} e^{-D\beta_m^2 t} + \frac{2}{a^2} \int_0^{\tau} \left\{ \frac{1}{s^{1/2}} \frac{I_1(s^{1/2})}{I_0(s^{1/2})} \right\} \sum_{m=1}^{\infty} \frac{e^{-D\beta_m^2 t}}{\beta_m^2} \right] \right\} \quad (6)$$

The operator  $\int_0^{\tau} \dots^{-1}$  indicates that the term following in brackets is to be inverted from transformed space (s) to direct space (t). For k = 0, the expression for f can be further simplified to read

The above inversions can be done either analytically or numerically. Thomas (2) performed the inversion

analytically leading to the imaginative numerical evaluation of the resulting double sum. The approach taken here will be to perform the inversion numerically using a general inversion technique which will now be described.

**Numerical Laplace Transform Inversion**

From the definition of the inversion of  $\bar{f}(s)$

$$f(t) = \frac{1}{2\pi i} \int_{\gamma-i\infty}^{\gamma+i\infty} ds e^{st} \bar{f}(s)$$

where  $\gamma$  is to the right of all singularities of  $\bar{f}$ , one can obtain (after some manipulation)

$$f(t) = \frac{2}{\pi t} e^{\gamma t} \int_0^{\infty} d\omega \operatorname{Re}[\bar{f}(\gamma + i\omega/t)] \cos \omega$$

By evaluating the integral as an infinite series over the half periods of the cosine, we find

$$f(t) = \frac{2}{\pi t} e^{\gamma t} \left\{ \int_0^{\pi/2} d\omega \operatorname{Re}[\bar{f}(\gamma + i\omega/t)] \cos \omega + \sum_{k=1}^{\infty} (-1)^k \int_{-\pi/2}^{\pi/2} d\omega \operatorname{Re}[\bar{f}(\gamma + i(\omega+k\pi)/t)] \cos \omega \right\} \quad (7)$$

The integrals in Eq. (7) are evaluated using a reliable and accurate Romberg integration scheme (3). If evaluated as presented, the alternating series would most likely converge very slowly making the inversion unusable. However, by applying the Euler-Knopp transformation for alternating series (3), the convergence is greatly accelerated and is the main reason for the effectiveness of this scheme. The major advantage of the above numerical inversion is that the singularities of  $\bar{f}(s)$  in the complex plane need not be explicitly known other than the rightmost singularity.

**Asymptotic Small Time Expressions**

In practice, the diffusivity  $D$  is very small ( $\sim 10^{-8}$   $\text{cm}^2/\text{s}$ ) and the above expression for  $f$  and  $g$  [Eq. (4), (5), (6)] become difficult to evaluate at small times. The infinite series in these expressions converges very slowly in this case. To overcome this numerical difficulty, asymptotic series for small times are obtained. The central relation used to obtain these series is (1)

$$\frac{\ell^2}{2} \sum_{m=1}^{\infty} \frac{e^{-D\beta_m^2 t}}{\beta_m^2} \sim 1 - \frac{2}{\sqrt{\pi}} \frac{a}{\ell} \sqrt{\tau} + O(e^{-1/\tau}), \quad \tau < < 1 \quad (8)$$

Equation (8) is then coupled with the asymptotic expression

$$\mathcal{L}^{-1} \left\{ \frac{1}{s^{3/2}} \frac{I_1(s^{1/2})}{I_0(s^{1/2})} \right\} \sim \frac{2}{\sqrt{\pi}} \sqrt{\tau} - \frac{\tau}{2} - \frac{\tau^{3/2}}{6\sqrt{\pi}} - \frac{\tau^2}{16} + O(\tau^{5/2})$$

to give

$$f(t,0) \sim b_0 \tau^{1/2} + b_1 \tau + b_2 \tau^{3/2} + b_3 \tau^2 + O(\tau^{5/2}) \quad (9a)$$

$$b_0 = \frac{2}{\sqrt{\pi}} \frac{a}{\ell} + \frac{4}{\sqrt{\pi}}$$

$$b_1 = 1 + \frac{8}{\pi} \frac{a}{\ell}$$

$$b_2 = \frac{2}{\sqrt{\pi}} \frac{a}{\ell} - \frac{1}{3\sqrt{\pi}}$$

$$b_3 = \frac{2}{3\pi} \frac{a}{\ell} - \frac{1}{8}$$

Note that  $b_2, b_3$  are incorrect in Nestor's formulation (1). Asymptotic expressions for the other quantities of interest are obtained from Eq. (9). For  $g(t,0)$  we have from Eq. (3b)

$$g(t,0) = \frac{df(t,0)}{dt} = \sum_{i=0}^3 \frac{(i+1)}{2} b_0 \tau^{(i-1)/2} + O(\tau^{3/2}) \quad (9b)$$

and  $g(t,k)$  is then obtained from the relation (2)

$$g(t,k) = e^{-kt} g(t,0) \quad (9c)$$

An expression for  $f(t,k)$  is found by noting that

$$\bar{f}(s,k) = \frac{s+k}{s} \bar{f}(s+k,0)$$

yielding

$$f(t,k) = e^{-kt} f(t,0) + k \int_0^t dt' e^{-kt'} f(t',0) \quad (9d)$$

and introducing Eq. (9a) for  $f$  into the integral. The integral can then be evaluated either analytically or using the Romberg integrator.

**Results**

Figures 2a,b are included to demonstrate the accuracy of the numerical Laplace transform inversion to characterize material migration in a cylindrical waste form. The relative error between the exact series ( $\epsilon$ ) representations (2)

$$f_e(t,0) = 1 - \frac{8}{\ell^2} \sum_{m=1}^{\infty} \frac{e^{-\beta_m^2 Dt}}{\beta_m^2} \sum_{n=1}^{\infty} \frac{e^{-j_{0,n}^2 Dt/a^2}}{j_{0,n}^2} \quad (10a)$$

$$g_e(t,0) = \frac{8D}{\ell^2} \sum_{m=1}^{\infty} \sum_{n=1}^{\infty} \left( \frac{1}{a^2 \beta_m^2} + \frac{1}{j_{0,n}^2} \right) e^{-(\beta_m^2 + j_{0,n}^2/a^2)Dt} \quad (10b)$$

where  $j_{0,n}$  is the  $n$ th zero of the zeroth order Bessel function, and the numerical inversion for several desired truncation ( $\epsilon_T$ ) and Romberg integration ( $\epsilon_R$ ) errors is presented ( $\epsilon_T = \epsilon, \epsilon_R = \epsilon/10$ ). The actual error is always less than the desired error indicating that for intermediate and large times, the numerical scheme will provide accurate results. For small times, or more precisely small values of  $\tau$ , the numerical inversion requires long computing times and the series requires many terms for convergence. Figure 3 presents a comparison of the asymptotic representation [Eq. (9a)] with  $f_e(t,0)$  for an increasing number of terms in the series representation. As is readily seen for small  $\tau$  many terms are required in the series evaluation to provide accurate results. Figure 4 gives the variation of  $f(t,k)$  with  $k$ . As anticipated, the fractional inventory approaches an equilibrium value less than 1 as  $k$  increases. This is a result of more material being retained in the waste form as  $k$  increases. Another measure of the algorithmic accuracy is that in comparison with the series evaluation, the equilibrium values given by the numerical inversion agree to five places. In Figs. 5a-c, the variations of height, radius and diffusivity are considered in order to demonstrate the use of the inversion and asymptotic representations as a tool for comparative analysis. As shown in Figs. 5a,b, increasing the radius allows more material to be released than for a corresponding increase in height because of the smaller area differential associated with changes in height. The leaching rate, shown in Fig. 5c, initially increases with increased diffusion but then at later times decreases with  $D$ .

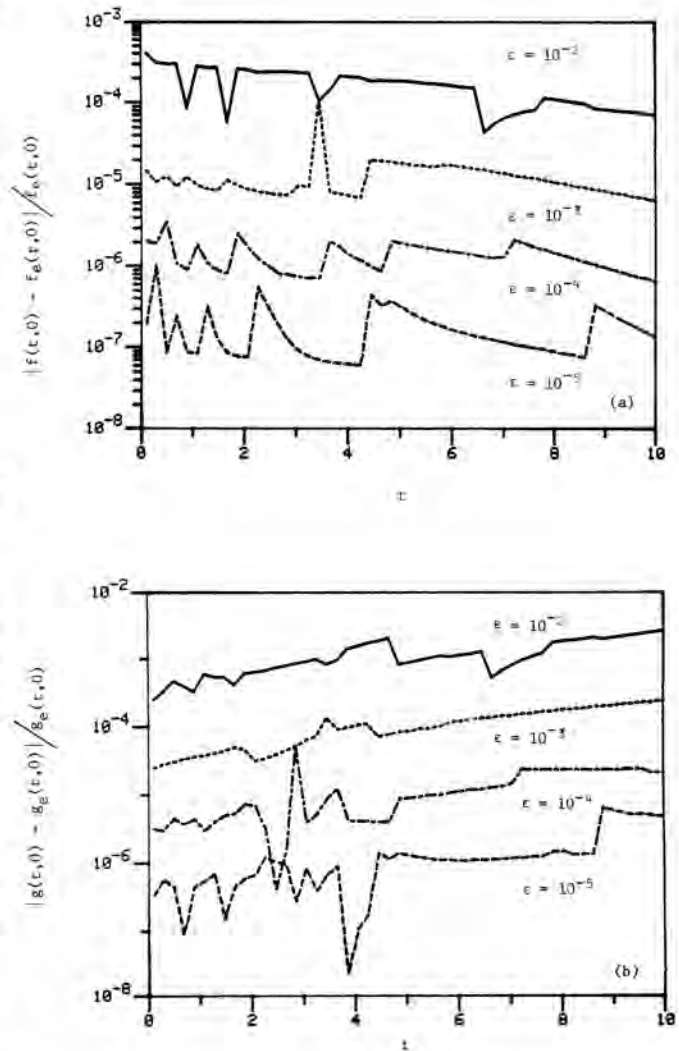


Fig. 2. Comparisons with Analytical Solution ( $k=0, D=0.05, a=\ell=1$ )

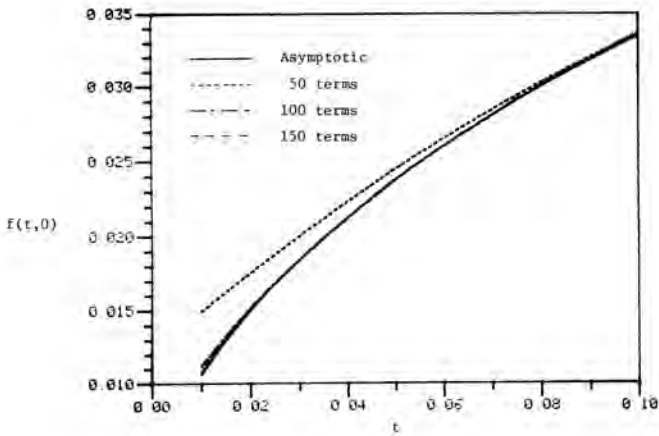


Fig. 3. Small Time Comparison ( $k=0, D=0.001, a = \ell = 1$ ).

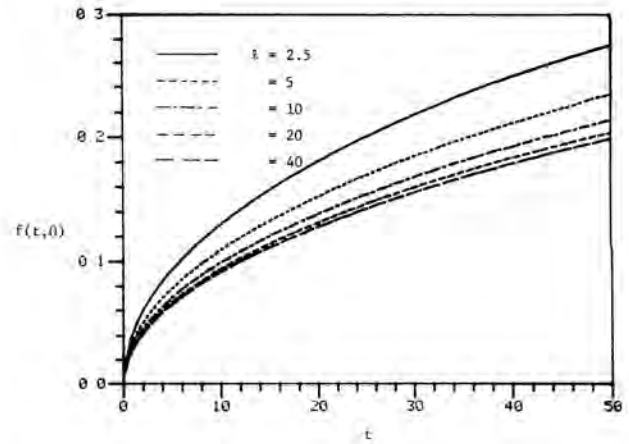


Fig. 5a. Comparison for Different Heights ( $D=0.001, k=0, a=2.5$ ).

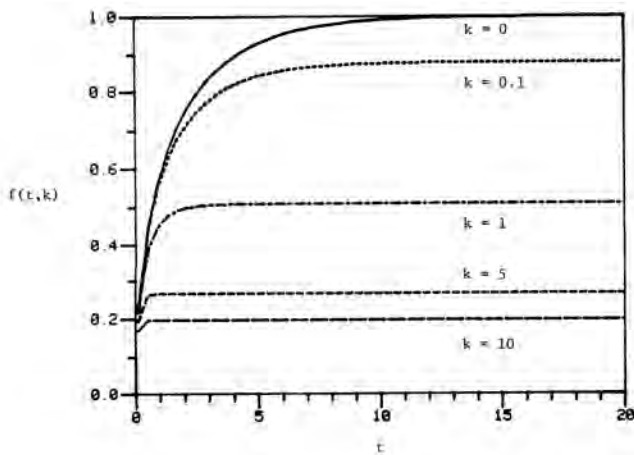


Fig. 4. Approach to Equilibrium for  $f(t,k)$  ( $D=0.05, a = \ell = 1$ ).

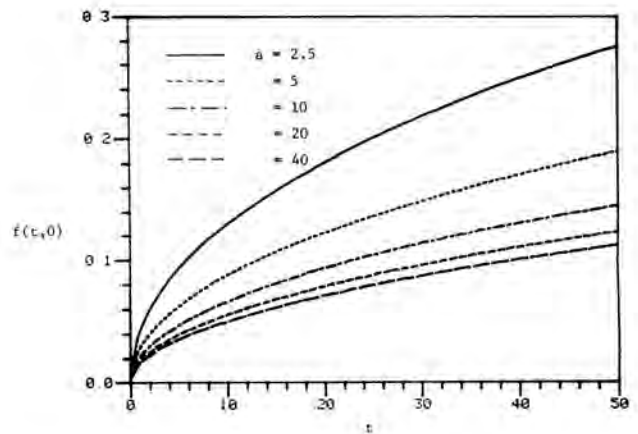


Fig. 5b. Comparison for Different Radii ( $D=0.001, K=0, \ell=2.5$ ).

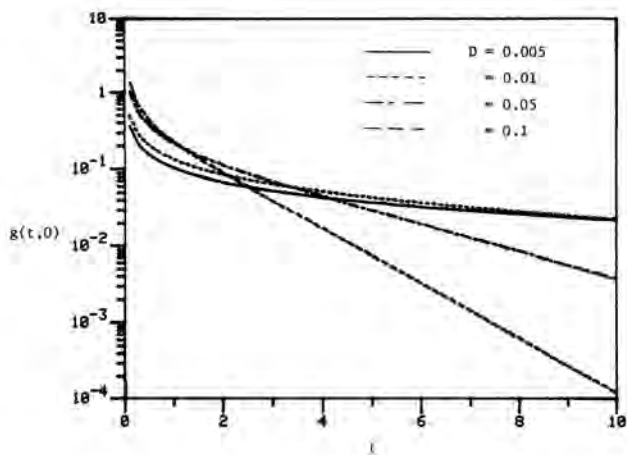


Fig. 5c. Variation of  $g(t,0)$  with  $D(a = l = 1)$ .

This behavior is a result of significant depletion of the diffusant for large  $D$  thus slowing down the diffusion process.

A final comparison has been made with  $C_s137$  release data from boric acid/cement composites (5). An attempt to match the analytical two parameter model ( $D,k$ ) with experimental data is shown in Figs. 6a-d for cylindrical waste forms of varying heights and diameters. The initial release is predominately controlled by diffusion while the later release is controlled by retention. For the values of  $D$  and  $k$  indicated, the model and experimental data are in agreement to within the experimental error (not shown). All cases but the last are predicted by similar parameters. Possibly the difference could be related to temperature effects which were not considered. In all cases, however, the model could be adjusted to fit the experimental results very closely. The model predictions are about a factor of three higher than those predicted by the semi-infinite/no retention model used in the experimental analysis of Ref. 5. The discrepancy may be a result of the crude semi-infinite/no retention model or due to initial non-diffusive processes controlling the release. Further investigation is needed to determine the origins of this discrepancy.

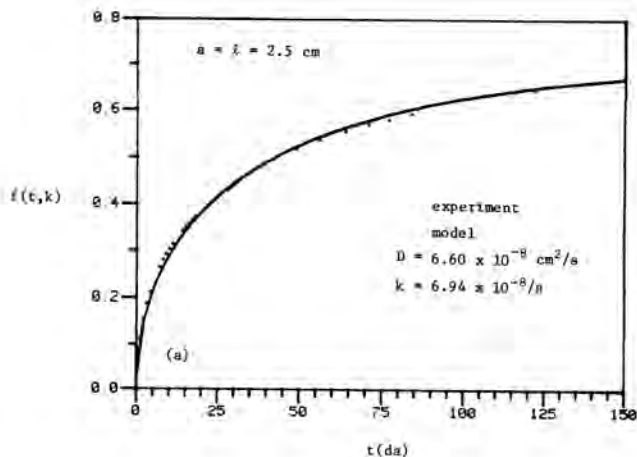


Fig. 6. Comparison of Model and Experiment.

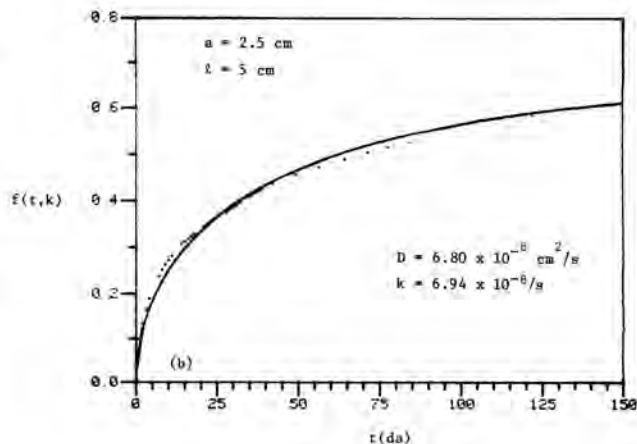


Fig. 6b.

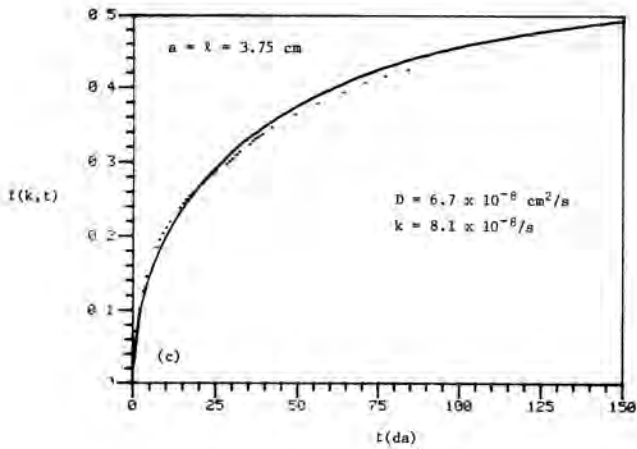


Fig. 6c.

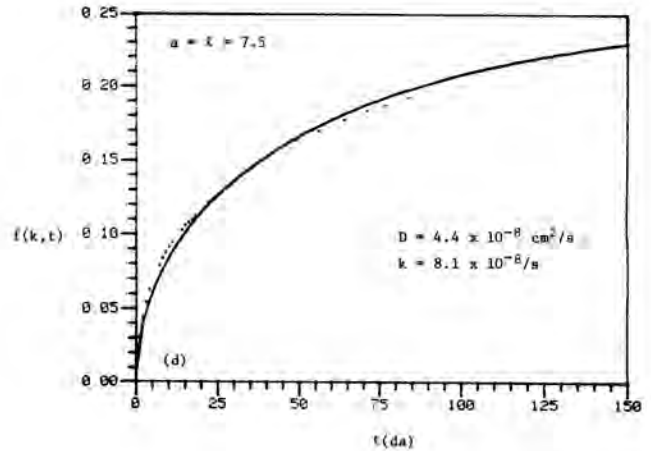


Fig. 6d.

**ACKNOWLEDGMENT**

I would like to acknowledge G. F. Thomas for providing me with several key references that enabled me to improve my presentation and understanding.

**REFERENCES**

1. C. W. Nestor, Jr., Diffusion From Solved Cylinders ORNL/CSD/TM-84, 1980.

2. G. F. Thomas, Ann. Nucl. Energy, V14, 283 (1987).  
 3. A. R. Miller, FORTTRAN Program for Scientists and Engineers, SYBEX, Berkeley, CA, 1982.  
 4. F. B. Hildebrand, Introduction to Numerical Analysis, McGraw-Hill, NY, 1956.  
 5. R. Dayal, H. Arora, and N. Marcos, NUREG/CR-3382, BNL-NUREG-51690, 1983.